OFFICE OF NAVAL RESEARCH

Contract N00014-91-J-1896

R & T Code 413q006

Technical Report No. 58

Dissociative Electron Attachment of O_2 : A Solid - State Effect on Potential Curve Crossing.

By

Dr. David E. Ramaker

Prepared for Publication

in

Surface Science

George Washington University
Department of Chemistry
Washington, D.C.

January, 1992

SECURITY CLASSIFICATION OF THIS PAGE

REPORT DOCUMENTATION PAGE

1a. REPORT SECURITY CLASSIFICATION Unclassified	1b. RESTRICTIVE MARKINGS
2a. SECURITY CLASSIFICATION AUTHORITY	3. DISTRIBUTION / AVAILABILITY OF REPORT Approved for public release; distribution unlimited
2b. DECLASSIFICATION / DOWNGRADING SCHEDULE	
4. PERFORMING ORGANIZATION REPORT NUMBER(S) Technical Report # 58	5. MONITORING ORGANIZATION REPORT NUMBER(S)
6a. NAME OF PERFORMING ORGANIZATION Dept. of Chemistry George Washington Univ. 6b. OFFICE SYMBOL (If applicable)	7a. NAME OF MONITORING ORGANIZATION Office of Naval Research (Code 418)
6c. ADDRESS (City, State, and ZIP Code) Washington, DC 20052	7b. ADDRESS (City, State, and ZIP Code) Chemistry Program 800 N. Quincy Street Arlington, VA 22217
8a. NAME OF FUNDING / SPONSORING ORGANIZATION Office of Naval Research 8b. OFFICE SYMBOL (If applicable)	9. PROCUREMENT INSTRUMENT IDENTIFICATION NUMBER Contract N00014-91-J-1896
8c. ADDRESS (City, State, and ZIP Code) Chemistry Program 800 Nth, Quincy, Arlington, VA 22217	10. SOURCE OF FUNDING NUMBERS PROGRAM ELEMENT NO. / PROJECT NO. / TASK NO. R & T 413q006 / WORK UNIT ACCESSION N

11. TITLE (Include Security Classification)

Dissociative Electron Attachment of O_2: a Solid-State Effect On Potential curve crossing.

12. PERSONAL AUTHOR(S)
Dr. Hideo Sambe and Dr. David E. Ramaker

13a. TYPE OF REPORT	13b. TIME COVERED	14. DATE OF REPORT (Year, Month, Day)	15. PAGE COUNT
Interim Technical	FROM _____ TO _____	January 1992	

16. SUPPLEMENTARY NOTATION

Prepared for publication in Surface Science

17. COSATI CODES			18. SUBJECT TERMS (Continue on reverse if necessary and identify by block number)
FIELD	GROUP	SUB-GROUP	

19. ABSTRACT (Continue on reverse if necessary and identify by block number)

Previously published data on electron stimulated desorption (ESD) from condensed O_2 or O_2 solid matrices are reanalyzed. In the gas phase, the O_2^- ($^2\Sigma_g^+$) resonant state at 8.5 eV is known to dissociate predominantly into the second lowest limit. In this paper we point out that this dissociation requires a non-adiabatic curve crossing. In the condensed phase or i solid matrices, this resonant state is found to dissociate adiabatically into the lowest lim as well as non-adiabatically into the second limit. Furthermore, we find that the branching ratio strongly depends on the kinetic energy of the dissociating atoms. The singlet excited oxygen atom, O* (^1D), formed upon dissociation into the second limit, is found to participat in an anion complex formation via incage recombination.

20. DISTRIBUTION / AVAILABILITY OF ABSTRACT	21. ABSTRACT SECURITY CLASSIFICATION
☒ UNCLASSIFIED/UNLIMITED ☒ SAME AS RPT. ☐ DTIC USERS	Unclassified
22a. NAME OF RESPONSIBLE INDIVIDUAL Dr. Mark Ross	22b. TELEPHONE (Include Area Code) (202) 696-4409
	22c. OFFICE SYMBOL

DD FORM 1473, 84 MAR

83 APR edition may be used until exhausted.
All other editions are obsolete.

SECURITY CLASSIFICATION OF THIS PAGE
Unclassified

Surface Science 00 (1992) SSC0172J
North-Holland

surface science

Dissociative electron attachment of O_2: a solid-state effect on potential curve crossing

Hideo Sambe and David E. Ramaker

Chemistry Department, George Washington University, Washington, DC 20052, USA

Received 10 September 1991; accepted for publication 30 September 1991

Previously published data on electron stimulated desorption (ESD) from condensed O_2 or O_2 in solid matrices are reanalyzed. In the gas phase, the $O_2^-(^2\Sigma_g^+)$ resonant state at 8.5 eV is known to dissociate predominantly into the second lowest limit. In this paper we point out that this dissociation requires a non-adiabatic curve crossing. In the condensed phase or in solid matrices, this resonant state is found to dissociate adiabatically into the lowest limit as well as non-adiabatically into the second limit. Furthermore, we find that the branching ratio strongly depends on the kinetic energy of the dissociating atoms. The singlet excited oxygen atom, $O^*(^1D)$, formed upon dissociation into the second limit, is found to participate in an anion complex formation via incage recombination.

1. Introduction

Recently, we performed a theoretical investigation of dissociative electron attachment (DEA) for O_2 and found that three O_2^- resonant states are sufficiently long lived to yield O^- anions [1]. We also found that one of these three O_2^- states can dissociate into two different dissociation limits, one limit requiring a non-adiabatic curve crossing. Based on this new information and the recent finding that desorption from a solid surface often involves a "bounce" trajectory and sometimes is quenched [2], we have reexamined previous interpretations of the experimental DEA data for O_2.

2. Theoretical background

Table 1 summarizes our previous theoretical findings concerning DEA of O_2. Of the many O_2^- states, only three states, i.e., $^2\Pi_u(1\pi_u^{-1}1\pi_g^2)$, $^2\Sigma_g^+(3\sigma_g^{-1}1\pi_g^2)$ and $^2\Sigma_u^+(2\sigma_u^{-1}1\pi_g^2)$, live long enough to produce dissociation yielding O^- anions. The other O_2^- states autoionize too fast and hence cannot yield O^- anions [1]. Furthermore,

Table 1
Summary of dissociative electron attachment mechanisms

Characteristics	Mechanism			
	I	II	III	IV
Symmetry of O_2^-	$^2\Pi_u$	$^2\Sigma_g^+$	$^2\Sigma_g^+$	$^2\Sigma_u^+$
Electronic configuration	$2\pi_u^{-1}1\pi_g^2$	$3\sigma_g^{-1}1\pi_g^2$	$3\sigma_g^{-1}1\pi_g^2$	$2\sigma_u^{-1}1\pi_g^2$
Vertical energy	6 eV	8 eV	9 eV	13 eV
Electron attachment to the ground state	Allowed	Forbidden	Forbidden	Forbidden
Lifetime against autoionization	Marginal for dissociation	Longer than $^2\Pi_u$	Longer than $^2\Pi_u$	Comparable to $^2\Sigma_g^+$
Dissociation limit	$O(^3P)+O^-$	$O(^3P)+O^-$	$O^*(^1D)+O^-$	$O^*(^1D)+O^-$
Initial direction of O^-	Towards surface	Away from surface	Towards surface	Towards surface

the autoionization lifetime of the $^2\Sigma_g^+$ and $^2\Sigma_u^+$ states are predicted to be longer than that of the $^2\Pi_u$ state [1].

The $^2\Sigma_g^+$ and $^2\Sigma_u^+$ states cannot be reached from the ground state ($^3\Sigma_g^-$) of O_2 via electron attachment, because of the σ^- selection rule [3]. To remove this restriction, the cylindrical symmetry of the O_2 molecule must be perturbed by its neighbors. The $^2\Sigma^+$ states can however be reached directly from the first excited state $O_2^*\,^1\Delta_g$ even in the gas phase. Such a process, namely,

$$e^- + O_2^*(^1\Delta_g) \rightarrow O_2^{-*}(^2\Sigma_g^+) \rightarrow O^*(^1D) + O^-(^2p), \qquad (1)$$

has been observed for gaseous O_2 and identified as such by Belic and Hall [4]. This $^2\Sigma_g^+$ state was observed at 8.5 eV vertically above the O_2 ground state, in line with its predicted vertical energy of 8.1 ± 0.9 eV [1]. This state is the lowest $^2\Sigma_g^+$ state of O_2^-.

According to the Wigner–Witmer correlation rule [5], the lowest $^2\Sigma_g^+$ state must dissociate adiabatically into the lowest limit [1]. However, Belic and Hall [4] found that the (lowest) $^2\Sigma_g^+$ state dissociates into the second lowest limit almost exclusively as indicated in eq. (1). This implies that the $^2\Sigma_g^+$ state must cross a curve in the dissociation terminating at the second lowest limit. The presence of a non-adiabatic curve crossing for the lowest $^2\Sigma_g^+$ state was previously indicated by us [1], but we did not expect such a high efficiency (almost 100%) for the non-adiabatic curve crossing. The O_2^- potential curves calculated by Michels [6] with the MCSCF method, which may be the most accurate curves available, also show an avoided curve crossing for the lowest $^2\Sigma_g^+$ state and suggest a high efficiency for the non-adiabatic curve crossing, because of the relative slopes of the two interacting curves and the small energy gap at the crossing region. To sum up, in the gas phase, the lowest $O_2^-(^2\Sigma_g^+)$ resonant state dissociates predominantly into the second lowest limit via a non-adiabatic curve crossing.

Now, the question arises: What happens when the O_2 molecules are condensed or placed in a matrix? Does the lowest $^2\Sigma_g^+$ state still dissociate predominantly into the second lowest limit, as it does in the gas phase? Is the non-adiabatic curve crossing sensitive to the solid environment? In the solid, the potential curves will be modified due to interaction of the dissociating atoms with their neighbours especially at larger internuclear distances; and furthermore the dissociating atoms will be slowed down by their neighbors, favoring the adiabatic process in the solid phase. Thus, we might expect that both the adiabatic and non-adiabatic dissociations would occur in the solid phase. The branching ratio between these two processes, according to the Landau–Zener theory of curve crossings [7], depends strongly (through an exponential function) on the velocity of the dissociating atoms, so that the lower and higher energy portions of the $^2\Sigma_g^+$ state might dissociate predominantly into the first and second lowest dissociation limits, respectively.

Each of the dissociation limits of the homonuclear O_2^- states is degenerate in the gas phase. This degeneracy will be removed, when the O_2^- rests on a polarizable surface with its symmetry axis non-parallel to the surface. For the non-parallel case, the O_2^- state can dissociate into either $O + O^-/S$ or $O^- + O/S$, where "S" indicates the surface. The $O + O^-/S$ limit is lower than the $O^- + O/S$ limit by the electronic polarization of the matrix due to the O^- anion. Regardless of the degeneracy, each O^-/Λ state must be connected uniquely to one of these limits. This connection between the O_2^- state and the dissociation limit can be determined by applying the Wigner–Witmer correlation and non-crossing rules [5]. The results obtained are shown in table 1. Dissociation into the $O + O^-/S$ or $O^- + O/S$ limit implies that the O^- anion moves towards or away from the surface respectively. The arguments given in this paragraph can also be applied to O_2 located in the bulk near a metal substrate. In this case, the image charge formed in the metal removes the degeneracy.

Desorbing anions may arise from DEA of O_2 molecules located in either the top or the second top layer of a film. Desorption initiated from the third layer is unlikely, especially for a 3 monolayer (ML) thick film deposited on a metal surface. The DEA of O_2 in the second layer will be

similar to the DEA of O_2 in a solid matrix. Hence, we expect "matrix" effects for O_2 molecules in the second layer, such as the in-cage recombination of the dissociating atoms [8]. Because of this recombination, DEA in the second layer can result in formation of a complex including both of the dissociating atoms and a neighboring molecule. In contrast, for the DEA of O_2 in the top layer, one of the dissociating atoms almost always leaves the film, and therefore a complex anion is formed that includes only the dissociating atom which initially moves towards the surface.

As indicated in table 1, we differentiate four mechanisms for the DEA of O_2 in a solid matrix. Mechanisms I–IV can be initiated by electron impact with energies around 6, 8, 9 and 13 eV respectively symmetry of the O_2 molecule must be perturbed by its neighbors. Except for mechanism II, the O^- anions produced by DEA move initially towards the surface requiring a bounce off the surface via a complex formation. Finally, mechanisms I and II produce the triplet oxygen atom $O(^3P)$, while mechanisms III and IV produce the excited singlet oxygen atom $O^*(^1D)$. Because of the Wigner spin-conservation principle [9], the singlet $O^*(^1D)$ atom is expected to be more reactive with neighboring singlet molecules than the triplet $O(^3P)$ atom.

3. Results from O_2 condensed on noble-gas films

3.1. Experimental results

The electron-stimulated desorption (ESD) of O^- anions from O_2 molecules condensed on a noble-gas (Ar, Kr or Xe) film has been studied extensively by Sanche's group. Some of their results have been published [10], although much of it is still unpublished. Fortunately, the unpublished data are also available to us. These O^- data show the following:

(a) When the O_2 coverage is low enough (that is, < 0.05 ML), a single peak appears around 6 eV in the O^- yield curve.

(b) As the O_2 coverage increases, new features (shoulder or peak) appear around 8 eV (shoulder or peak) and 14 eV (peak) and increase in intensity relative to the 6 eV peak.

(c) The intensity ratio, (6 eV peak)/(8 eV peak), for a fixed O_2 coverage increases in the order of Xe < Kr < Ar.

(d) When O_2 (0.17 ML) is condensed on a 20 ML Xe film which was condensed at 17 K, a single peak appears at 6.5 eV in the O^- yield curve. However, when the same amount of O_2 is condensed on a 20 ML Xe film which was condensed at 40 K, all three features appear at 6.5, 8 and 14 eV.

3.2. Interpretation

We interpret these trends as follows:

Items (a) and (b) indicate that the 6 eV peak arises from the symmetry-allowed mechanism I and the features around 8 and 14 eV arise from symmetry-forbidden mechanisms II and IV, respectively. (Previously [10], we attributed the 8 eV feature to a coherent scattering of the incident electron by a well-ordered (noble-gas) film.)

Items (a) and (d) imply that electron attachment to isolated O_2 molecules in noble-gas matrix is still forbidden, like O_2 in the gas phase. In other words, an association of another O_2 is required in order to perturb the cylindrical symmetry of O_2 in noble-gas matrices. As an explanation of item (d), we speculate that Xe films condensed at 17 K have a rougher surface than those condensed at 40 K and O_2 molecules condensed on the rougher surface tend to be more isolated from each other.

In the above experiments, a majority of the O_2 molecules rest on the surface of the noble-gas film. The O^- anions produced by mechanisms I, III and IV, initially move towards the surface requiring them to "bounce" off the surface to be observed. In contrast, O^- anions produced by mechanism II move directly away from the surface. The O^- yield via this direct mechanism (II) should be less dependent on the film than those via the indirect "bounce" mechanism (I). The intensity ratio, peak(I)/peak(II), therefore, should give an indication for the "bouncing" efficiency. On these grounds, the observed order in (c) implies that the Ar film is the best "bouncer"

of O^- anions. The ordering in (c) correlates with the interaction strengths between O^- anions and the rare gases: that is, the weaker the interaction, the more efficient the bouncing.

4. Results from condensed pure and mixed gases

4.1. Experimental results

Figs. 1–4 compare the ESD yields of O^- or OH^- anions from various molecular solids containing O_2. For comparison purposes, we have shown spectra (c) and (d) more than once in figs. 1–3. In order to focus our attention on mechanisms I–III, the energy range of the incident

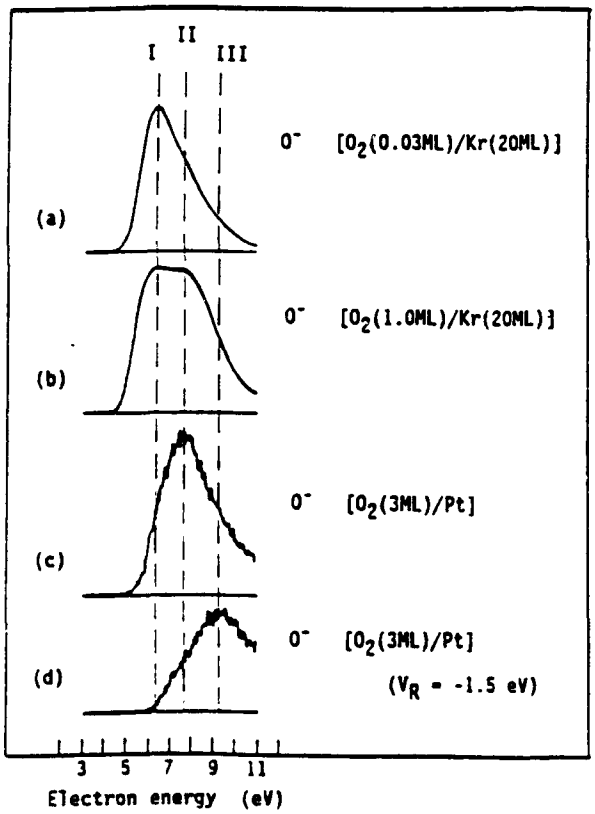

Fig. 1. ESD O^- yields from O_2 (3 ML) films and O_2 condensed on Kr are plotted as a function of the incident electron energy. Spectrum (d) is measured with a potential ($V_R = -1.5$ eV) retarding the desorbing O^- anions. Spectra (a) and (b) are taken from ref. [10], and spectra (c) and (d) are from ref. [11].

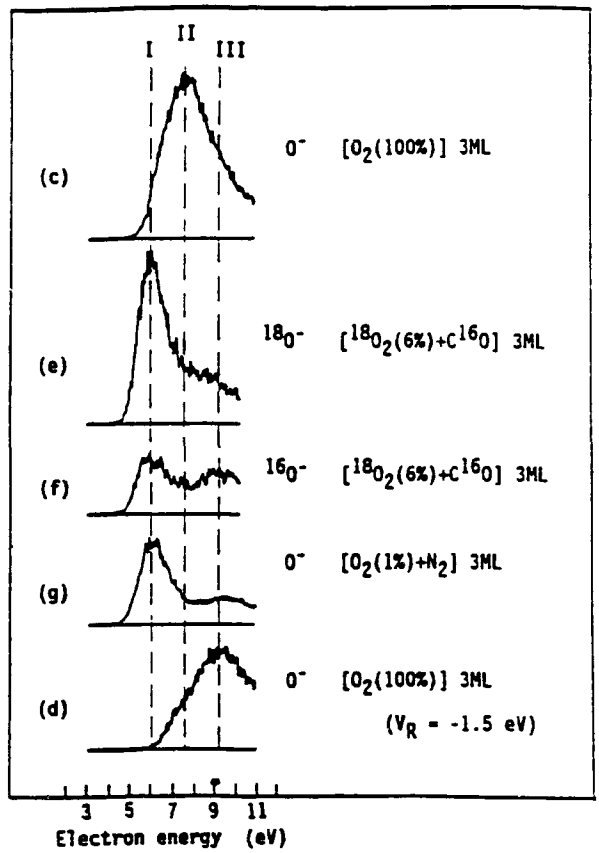

Fig. 2. ESD O^- yields from 3 ML films of ($^{18}O_2 + C^{16}O$) and ($O_2(1\%) + N_2$) mixtures are plotted as a function of the incident electron energy. Spectra (c) and (d) in this figure are identical to those in fig. 1. Spectra (e) and (f) are taken from ref. [12], and spectrum (g) is from ref. [13].

electron is limited to 11 eV. All spectra have been measured by Sanche and coworkers over several years and have been published in several papers.

The samples, except for spectra (a) and (b), are prepared by condensing a gas or a mixture of gases (as indicated in the figures, where % means volume percent) on a Pt substrate maintained at a temperature around 20 K. Samples for spectra (a) and (b) are prepared by first condensing 20 ML of Kr gas on a Pt substrate followed by condensation of (0.03 or 1.0 ML) O_2 gas. The thickness of the deposited films are estimated by the gas-volume expansion procedure. The electron beam is incident at an angle of 40° (or 30°) from the Pt surface. A portion of the desorbing

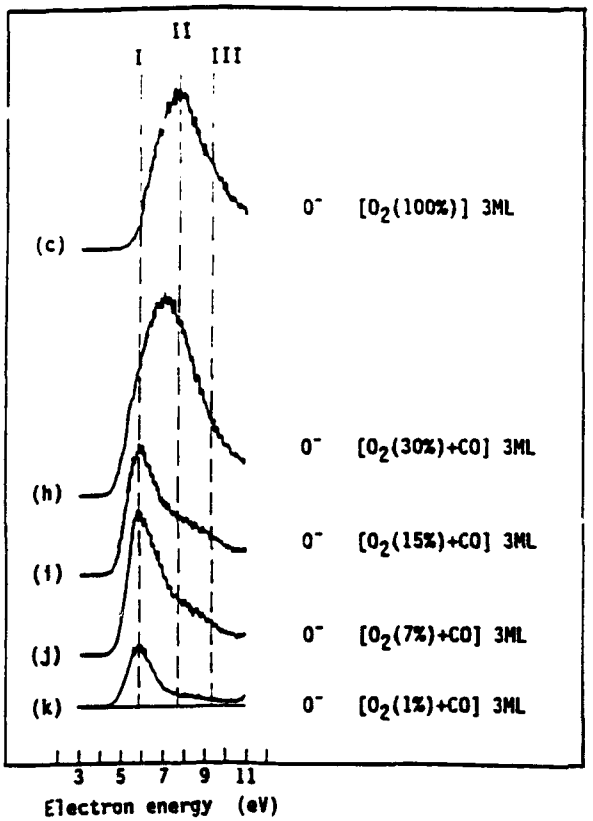

Fig. 3. ESD O^- yields from 3 ML films of $(O_2 + CO)$ mixtures with varying O_2 concentrations as indicated are plotted as a function of the incident electron energy. Spectra (h)–(k) are taken from ref. [13]. Spectrum (c) in this figure is identical to (c) in fig. 1.

anions are focused by ion lenses positioned at 70° from the Pt surface, mass analyzed, and counted as a function of the incident electron energy. Spectra (d) and (q) are measured with a potential ($V_R = -1.5$ or -1.8 eV) retarding the desorbing O^- anions. A slight difference between spectra (c) and (l) is due to different set ups for the ion-lens focusing [11]. We refer to individual papers for details. The reference number for each individual spectrum is given in the figure caption.

Spectra (e) and (f) show respectively $^{18}O^-$ and $^{16}O^-$ yields from a 3 ML film of $[^{18}O_2(6\%) + C^{16}O]$. The $^{16}O^-$ anions do not arise from the DEA of $C^{16}O$ molecules, because CO molecules are transparent in electron impact for the electron energies between 4.0 and 10.5 eV [16]. These $^{16}O^-$ anions arise from the DEA of $^{18}O_2$ molecules via a complex formation with $C^{16}O$. For the same reason, in spectra (h)–(k), the O^- anions from $[O_2 + CO]$ mixtures also arise from the DEA of O_2.

The OH^- anions from a mixture of oxygen and hydrocarbons in spectra (m)–(p) could arise from DEA of the hydrocarbons. The OH^- yield curves, however, resemble the O^- yield curves from O_2 and do not resemble the H^- or CH_n^- yield curves from hydrocarbons, which have a single peak around 10 eV [14]. Therefore, as concluded by Sanche and Parenteau [15], the OH^- anions are also attributable to the DEA of O_2.

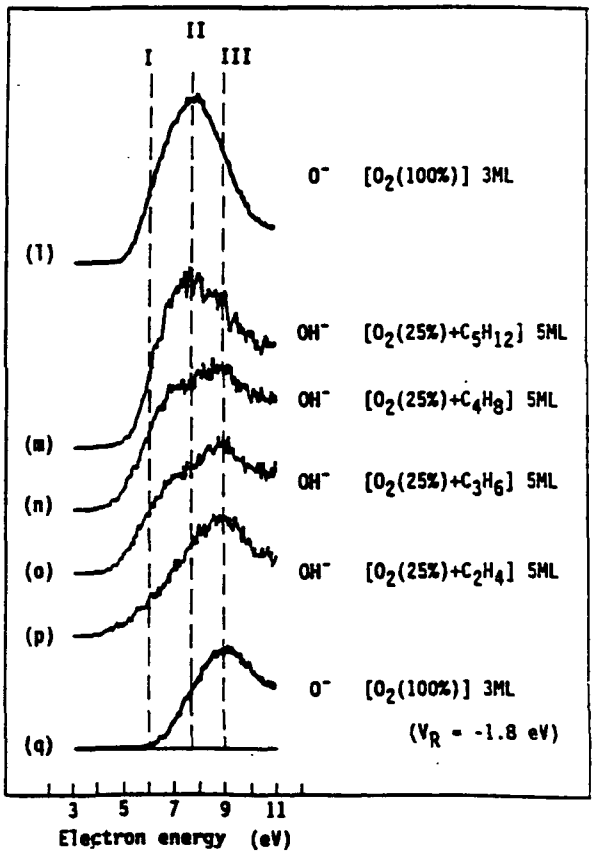

Fig. 4. ESD OH^- yields from 5 ML films containing O_2 (25 vol%) and the indicated hydrocarbon are plotted as a function of the incident electron energy. For comparison, ESD O^- yields from a (3 ML) O_2 film with and without a retarding potential ($V_R = -1.8$ eV) are also shown. The spectra (l) and (q) are obtained from ref. [14]. Spectra (m)–(p) are taken from ref. [15].

In short, all features observed in the spectra of figs. 1–4 arise from the DEA of O_2. The differences in the polarizabilities of Kr, N_2, CO and O_2 is small enough (± 0.1 eV) to be ignored for direct comparisons of these spectra.

4.2. Interpretations

Mechanism I is the only symmetry-allowed mechanism and is expected to appear around 6 eV. Furthermore, from a study of O_2/(noble gas) systems (see section 3), we have learned that an association of neighboring O_2 is required to observe the symmetry-forbidden mechanisms. Consequently, when the O_2 concentration in the film becomes low, a peak due to the symmetry-allowed mechanism dominates such as in spectra (a), (e), (g) and (k). Clearly these 6 eV peaks result from mechanism I.

The principal peak in spectrum (c) has also been attributed to mechanism I in all previous work (including some of our previous papers). This peak, however, aligns with the second feature of spectrum (b) at 8 eV, which corresponds to the symmetry-forbidden mechanism II, as seen in fig. 1.

The sequence of spectra (k) to (c) in fig. 3 might suggest that the peak position simply shifts to higher energy as the O_2 concentration increases and therefore might indicate that the principal peaks in spectra (k) and (c) arise from the same mechanism. Upon closer look, however, the peak in spectrum (h) is broader than the peak in (i) or (c); the threshold energy of (h) is the same as those of spectra (k)–(i) but lower than that of (c); and the peak position does not shift from (k) to (i). Furthermore, spectra (j)–(h) also appear to consist of two contributions peaked around 6 and 8 eV.

The sequence of spectra (a)–(c) is an analogue to the above-mentioned sequence of (k)–(c), since in both sequences the O_2 concentration increases. Again, two contributions are clearly seen in the intermediate spectra (b). Because both (6 and 8 eV) peaks are observed in spectra (j)–(h) and (b), the 8 eV peak cannot be a shifted peak of the 6 eV peak.

Arguments presented in the preceding three paragraphs strongly suggest that the principal peak in (c) is due to the symmetry-forbidden mechanism II. Moreover, figs. 1–3 indicate that spectrum (c) contains a very small contribution from the symmetry-allowed mechanism I. This is consistent with our theoretical model: The O^- anions produced via mechanisms I and III initially move towards the film surface, and most of them do not come out of the film because of the stronger O^-–O_2 interaction. On the other hand, the O^- anions produced via mechanism II move directly away from the surface. Therefore, the stronger peak will be due to mechanism II.

The theoretical model described above also predicts that the intensity due to mechanism I decreases relative to that of mechanism II, as the percentage of O_2 increases in the mixture. The spectra in fig. 3 are consistent with this prediction. The spectra (m)–(g) in fig. 4 also agree with this prediction, since the mixtures have large per-

Table 2
Proposed mechanisms IIIa–d for formation of anion complexes initiated by $O^*(^1D)$ attack
(i) $O^*(^1D)$ reacts with a neighboring molecule and forms a hot complex (kinetic energy of the $O^*(^1D)$ is incorporated into the complex); on the other hand, O^- colliding with neighbors loses its kinetic energy and remains in the cage.
(ii) The thermalized O^- reacts with the hot complex and forms a hot complex anion.
(iii) The hot complex anion decays yielding O^-, OH^-, or other anions. When the hot complex anion is on the surface, these anions desorb provided that they have kinetic energy larger than the surface-polarization energy.

	(i)		(ii)		(iii)		
$O^- + O^*(^1D) + O_2$	→	$O^-(\text{thermal}) + O_3^*$	→	O_4^{-*}	→	$O_3 + O^-$	IIIa
$O^- + O^*(^1D) + N_2$	→	$O^-(\text{thermal}) + N_2O^*$	→	$N_2O_2^{-*}$	→	$N_2O + O^-$	IIIb
$O^- + O^*(^1D) + CO$	→	$O^-(\text{thermal}) + CO_2^*$	→	CO_3^{-*}	→	$CO_2 + O^-$	IIIc
$O^- + O^*(^1D) + C_2H_4$	→	$O^-(\text{thermal}) + C_2H_4O^*$	→	$C_2H_4O_2^{-*}$	→	$C_2H_3O + OH^-$	IIId

centages (25%) of O_2 and the spectra consequently contain small contributions from mechanism I.

The 9 eV peak appears repeatedly in spectra (d), (f) and (g) of fig. 2 and also in spectra (n)–(q) of fig. 4. Our proposed mechanism for the origin of the 9 eV peaks is shown in table 2. Briefly the 9 eV peak originates from DEA of O_2 by mechanism III followed a complex formation initiated by $O^*(^1D)$. The sequence of reactions for forming a hot complex anion is proposed as follows: The DEA of O_2 via mechanism III produces O^- and $O^*(^1D)$ in a solid matrix. The $O^*(^1D)$ atom reacts with a neighboring molecule and forms a hot complex incorporating most of the $O^*(^1D)$ kinetic energy into the complex. On the other hand, the O^- anion being less reactive does not form a complex and loses its kinetic energy by colliding with neighbors. This thermalized O^- anion stays in the neighborhood and eventually reacts with the hot complex and forms a hot negative complex. When this negative complex decays, an O^- or OH^- anion is produced. In the following four paragraphs, we will show that this mechanism is consistent with the characteristics observed for the 9 eV peaks.

Comparison of spectra (d) and (q) reveals that a retardation potential of -1.5 and -1.8 eV makes almost no difference in the spectra. This indicates that the O^- anions measured in these spectra have kinetic energy significantly higher than 1.8 eV. This energetic O^- anion cannot be produced directly via mechanism II or III nor indirectly via simple complex formation involving the O^- alone,

$$O^- + O_2 \rightarrow O_4^{-*} \rightarrow O_2 + O^-. \quad (2)$$

We will show elsewhere [17] that only complex formation involving both $O^*(^1D)$ and O^-, as shown in table 2, is consistent with the observed maximum kinetic energies and threshold energies. The extra kinetic energy arises in part from the conversion of $O^*(^1D)$ electronic excitation energy to ion kinetic energy.

The reaction of $O^*(^1D)$ with hydrocarbons in liquid argon has been investigated by DeMore [18]. The rates of $O^*(^1D)$ attack on alkanes were found to be proportional to the number of C–H bonds present; furthermore the rate of $O^*(^1D)$ attack on the C=C double bond was found to be five times faster than that on the C–H bond. Based on these findings, we interpret spectra (m)–(p) in fig. 4. Spectrum (m) for the saturated hydrocarbon C_5H_{12} resembles spectrum (1) for the pure O_2, because the OH^- anions mainly result from the simple complex formation initiated by O^-, namely

$$O^- + C_5H_{12} \rightarrow C_5H_{12}O^{-*} \rightarrow C_5H_{11} + OH^- \quad (3)$$

as proposed by Sanche and Parenteau [15]. Spectra (n)–(p) for the unsaturated hydrocarbons reveal that the 9 eV contribution increasingly dominates as the ratio of the C=C bond to the C–H bonds increases. This is because the 9 eV contribution arises from mechanism IIId (see table 2), which is initiated by $O^*(^1D)$ attack on the C=C bond.

The collisional decay rates of $O^*(^1D)$ with N_2, O_2 and CO should correlate with the rates of complex formation with these molecules. It has been found [19] that the collisional decay rates of $O^*(^1D)$ are in the order of $N_2 > O_2 > CO$. This explains why the 9 eV peak is more visible in spectrum (g) for N_2 than in spectrum (k) for CO. It should be noted that the O_2 concentrations of these spectra are the same.

The 9 eV peak is also highly visible in spectrum (f). In this case, the $^{16}O^-$ anions cannot arise directly from the DEA of $^{18}O_2$. The $^{18}O^-$ anion from the DEA of $^{18}O_2$ must necessarily form a complex with $C^{16}O$ to yield the $^{16}O^-$ anion. Azria et al. [12] proposed again the simple O^- initiated complex formation mechanism for production of the $^{16}O^-$ anions, that is

$$^{18}O^- + C^{16}O \rightarrow {}^{18}OC^{16}O^{-*} \rightarrow {}^{18}OC + {}^{16}O^-. \quad (4)$$

The 6 eV peak in spectrum (f) may be due to this mechanism, where the $^{18}O^-$ anion is produced via mechanism I. However, we assign the 9 eV peak to the alternative $O^*(^1D)$ initiated complex formation mechanism, namely mechanism IIIc, based on the following grounds. The kinetic energy of $^{18}O^-$ anions produced by mechanisms I and III are comparable around 2 ± 0.1 eV. Further, the $^{18}O^-$ anions move towards the surface in both cases. The number of $^{18}O^-$ anions pro-

duced via these mechanisms, however, will be dramatically different, especially for a mixture with a small O_2 concentration, because mechanism III is after all symmetry forbidden while mechanism I is symmetry allowed. Consequently, if the $^{16}O^-$ anions at 6 and 9 eV were produced via the same O^- initiated complex formation mechanism, eq. (4), then the $^{16}O^-$ yield via mechanism I (at 6 eV) would be one or two orders of magnitudes larger than the $^{16}O^-$ yield via mechanism III (at 9 eV), contrary to the observed spectrum of (f).

Finally, anion complex formation via mechanisms IIIa–d must proceed in the bulk, so that the initial DEA of O_2 must occur in the second or deeper layer. Because, if the DEA of O_2 occurs in the top layer, one of the dissociating atoms leaves the film. Further, the resulting anion complex must be located on the surface so that decay products (such as O^- and OH^-) of the complex can desorb. This imposes a stronger condition that the initial DEA of O_2 must occur in the second layer.

5. Summary

Most of the features and characteristics observed for the ESD of O^- or OH^- anions from condensed O_2 or O_2 in solid matrices are found to be consistent with our proposed mechanisms summarized in table 1. The new findings include the following. In the gas phase, the $O_2^-(^2\Sigma_g^+)$ resonant state dissociates predominantly into the second lowest limit via a non-adiabatic curve crossing. In the condensed phase, this state dissociates adiabatically into the lowest limit as well as non-adiabatically into the second limit. DEA of O_2 via the $O_2^-(^2\Pi_u)$ resonant state (the principal gas-phase mechanism) is suppressed in the ESD of O^- from condensed O_2. The 9 eV peaks arise from complex formation initiated by $O^*(^1D)$ attack on neighboring molecules.

Acknowledgments

We thank Dr. L. Sanche for permission to quote his unpublished results, items (b) and (c) in section 3.1. This work was supported in part by the US Office of Naval Research.

References

[1] H. Sambe and D.E. Ramaker, Phys. Rev. 40 (1989) 3651.
[2] H. Sambe and D.E. Ramaker, in: Desorption Induced by Electronic Transitions DIET IV, Eds. G. Betz and P. Varga (Springer, Berlin, 1990) p. 251.
[3] H. Sambe and D.E. Ramaker, Chem. Phys. Lett. 139 (1987) 386.
[4] D.S. Belic and R.I. Hall, J. Phys. B 14 (1981) 365.
[5] E. Wigner and E.E. Witmer, Z. Phys. 51 (1928) 859.
[6] H.H. Michels, Adv. Chem. Phys. 45 (1981) 225.
[7] See for an example: K.J. Laidler and K.E. Shuler, Chem. Rev. 48 (1951) 153.
[8] V.E. Bondybey, in: Chemistry and Physics of Matrix-Isolated Species, Eds. L. Andrews and M. Moskovits (North-Holland, Amsterdam, 1989) p. 107.
[9] E. Wigner, Gottinger Nachrichten (1927) 376.
[10] H. Sambe, D.E. Ramaker, L. Parenteau and L. Sanche, Phys. Rev. Lett. 59 (1987) 505.
[11] R. Azria, L. Parenteau and L. Sanche, Phys. Rev. Lett. 59 (1987) 638.
[12] R. Azria, L. Parenteau and L. Sanche, Chem. Phys. Lett. 171 (1990) 229.
[13] R. Azria, L. Sanche and L. Parenteau, Chem. Phys. Lett. 156 (1989) 606.
[14] L. Sanche and L. Parenteau, Phys. Rev. Lett. 59 (1987) 136.
[15] L. Sanche and L. Parenteau, J. Chem. Phys. 93 (1990) 7476.
[16] L. Sanche and M. Michaud, Phys. Rev. B 30 (1984) 6078.
[17] H. Sambe and D.E. Ramaker, to be published.
[18] W.B. DeMore, J. Phys. Chem. 73 (1969) 391.
[19] R.J. Donovan and D. Husain, Chem. Rev. 70 (1970) 489.

TECHNICAL REPORT DISTRIBUTION LIST - GENERAL

Office of Naval Research (2)*
Chemistry Division, Code 1113
800 North Quincy Street
Arlington, Virginia 22217-5000

Dr. James S. Murday (1)
Chemistry Division, Code 6100
Naval Research Laboratory
Washington, D.C. 20375-5000

Dr. Robert Green, Director (1)
Chemistry Division, Code 385
Naval Weapons Center
China Lake, CA 93555-6001

Dr. Eugene C. Fischer (1)
Code 2840
David Taylor Research Center
Annapolis, MD 21402-5067

Dr. Elek Lindner (1)
Naval Ocean Systems Center
Code 52
San Diego, CA 92152-5000

Commanding Officer (1)
Naval Weapons Support Center
Dr. Bernard E. Douda
Crane, Indiana 47522-5050

Dr. Richard W. Drisko (1)
Naval Civil Engineering
Laboratory
Code L52
Port Hueneme, CA 93043

Dr. Harold H. Singerman (1)
David Taylor Research Center
Code 283
Annapolis, MD 21402-5067

Chief of Naval Research (1)
Special Assistant for Marine
Corps Matters
Code 00MC
800 North Quincy Street
Arlington, VA 22217-5000

Defense Technical Information
Center (2)
Building 5, Cameron Station
Alexandria, VA 22314

* Number of copies to forward